

Li_{1.1}(Zn_{1-x}Cr_x)As: Cr doped I-II-V Diluted Magnetic Semiconductors in Bulk Form

Quan Wang¹, Huiyuan Man¹, Cui Ding¹, Xin Gong¹, Shengli

Guo¹, Huike Jin¹, Hangdong Wang², Bin Chen², F.L. Ning^{1,*}

¹*Department of Physics, Zhejiang University, Hangzhou 310027, China and*

²*Department of Physics, Hangzhou Normal University, Hangzhou 310016, China*

(Dated: July 9, 2018)

We report the synthesis and characterization of bulk form diluted magnetic semiconductors I-II-V Li_{1.1}(Zn_{1-x}Cr_x)As ($x = 0.03, 0.05, 0.10, 0.15$) with a cubic crystal structure identical to that of III-V GaAs and II-VI zinc-blende ZnSe. With p -type carriers created by excess Li, 10% Cr substitution for Zn results in a ferromagnetic ordering below $T_C \sim 218$ K. Li(Zn,Cr)As represents another magnetic semiconducting system with the advantage of decoupling carriers and spins, where carriers are created by adding extra Li and spins are introduced by Cr substitution for Zn.

PACS numbers: 75.50.Pp, 71.55.Ht, 76.75.+i

The observation of ferromagnetic ordering in III-V (Ga,Mn)As [1] thin-film has generated extensive research into diluted magnetic semiconductors (DMS) [2–4]. The highest Curie temperature, T_C , has been reported as ~ 200 K with Mn doping levels of $\sim 12\%$ in (Ga,Mn)As [5, 6]. The application of spintronics may become possible once T_C reaches room temperature [4]. However, the research is hindered by two inherent difficulties: one is that the mismatch of valences of Ga³⁺ and Mn²⁺ prohibits the fabrication of bulk form specimens with higher Mn doping levels; the other is that it is difficult to determine precisely the amount of Mn that substitutes Ga, which donates a hole and acts as a local moment, since some Mn impurities enter interstitial sites [2]. In the II-VI family of DMS, i.e., (Zn_{1-x}Mn_x)Se, the chemical solubility can be as high as 70% and bulk form specimens are available [7, 8]. The isovalent substitution of Mn for Zn, however, makes it difficult to control the carrier density [9, 10], which is as low as 10^{17} cm⁻³, and the magnetic moment size is as small as $0.01 \mu_B/\text{Mn}$ [8, 11].

To overcome the difficulties encountered in III-V and II-VI DMS, Masek et al proposed that I-II-V direct-gap semiconductor LiZnAs may be a good candidate for fabrication of next generation of DMS [12]. LiZnAs is a direct gap semiconductor with a band gap of 1.6 eV [13]. It has a cubic structure, similar to that of zinc-blende GaAs and ZnSe, as shown in Fig. 1. More interestingly, if we view the combination of (Li¹⁺Zn²⁺) as Ga³⁺, (LiZn)As becomes GaAs; alternatively, if we view the combination of (Li¹⁺As³⁻) as Se²⁻, Zn(LiAs) becomes ZnSe. The I-II-V semiconductor LiZnAs shares some common characteristics with both III-V and II-VI semiconductors, and has two superior advantages from the view of synthesis: (1) the isovalent substitution of Mn for Zn overcomes the small chemical solubility; (2) the carrier density can be controlled by off-stoichiometry of Li concentrations.

Recently, Deng et al. successfully synthesized two bulk I-II-V DMS systems, Li(Zn,Mn)As [14] and Li(Zn,Mn)P

[15], with $T_C \sim 50$ K. The availability of the bulk form specimens readily enables the microscopic investigation of DMSs based on typical bulk probes of magnetism, such as nuclear magnetic resonance (NMR), muon spin relaxation (μSR) and neutron scattering, which would provide unique microscopic information of the ferromagnetism. For example, through the NMR measurement of local static and dynamic susceptibility at Li sites, Ding et al found that Mn atoms are homogeneously doped in Li(Zn,Mn)P, and Mn spin-spin interactions extend over many unit cells, which explains why DMSs could exhibit a relatively high T_C with such a low density of Mn [16].

Very recently, three other bulk DMS systems with decoupling of carriers and spins have been reported. Ding et al reported the successful fabrication of a new bulk “1111” DMS material, (La_{1-x}Ba_x)(Zn_{1-x}Mn_x)AsO, with T_C up to 40 K [17]; Yang et al reported the ferromagnetic ordering at 210 K for Sr and Mn doped LaO-CuS system [18]; Zhao et al. reported another ferromagnetic DMS system, (Ba,K)(Zn,Mn)₂As₂ with T_C up to ~ 180 K [19]. The Curie temperature of the latter two bulk DMSs is already comparable to that of thin film (Ga,Mn)As [5, 6].

In addition to Mn, magnetic Cr atoms have also been extensively doped into various III-V and II-VI semiconductors for fabrication of DMSs. For example, room temperature ferromagnetism has been observed in (Zn,Cr)Te thin films [20]. On the other hand, the Curie temperature T_C is relatively low, i.e., ~ 10 K in Cr doped GaAs [21–23]. The reason for such different T_C values between III-V and II-VI DMSs is still largely unknown. Furthermore, the electron configuration of Cr atom is $(3d)^5(4s)^1$, leaving the controversy about the valence of Cr and its spin state [21–24]. This situation is in contrast with the case of Mn²⁺ whose “+2” valence and high spin state have been widely accepted.

In this letter, we report the synthesis and characterization of Cr doped Li(Zn,Cr)As semiconductors. The carriers are introduced by excess 10% Li, and the spins are introduced by the substitution of Cr for Zn, respectively. We found that 3% Cr doping induces local moments, but no ferromagnetic ordering is formed. At the

*Electronic address: ningfl@zju.edu.cn

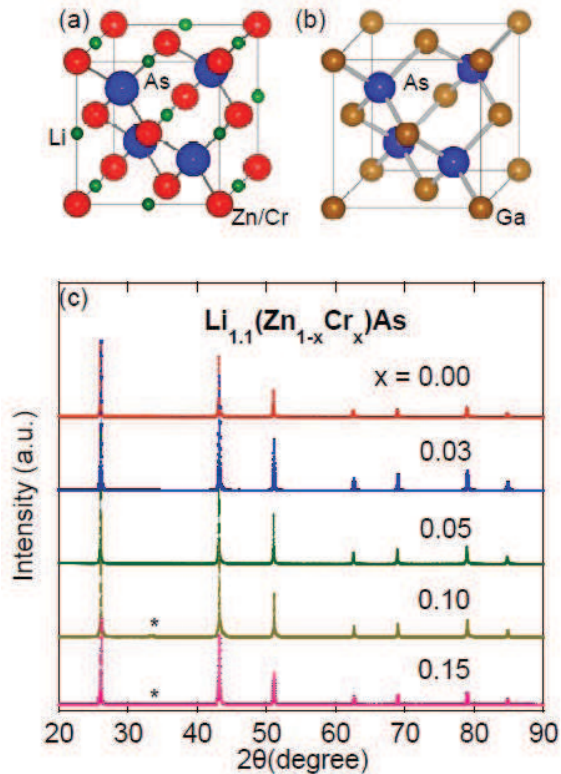


FIG. 1: (Color online). The crystal structure of (a) $\text{Li}(\text{Zn,Cr})\text{As}$, and (b) GaAs . (c) X-ray diffraction pattern of $\text{Li}_{1.1}(\text{Zn}_{1-x}\text{Cr}_x)\text{As}$. Traces of impurity CrAs (*) are marked for $x \geq 0.1$.

doping level of 5%, a ferromagnetic ordering is developed, as evidenced by a sudden enhancement of magnetization, and the parallelogram-shaped hysteresis loops below $T_C \sim 106$ K. T_C is maximized to ~ 218 K with 10% Cr doping, and decreases to 201 K at the doping level of 15%.

We synthesized the polycrystalline specimens $\text{Li}_{1.1}\text{Zn}_{1-x}\text{Cr}_x\text{As}$ ($x = 0.03, 0.05, 0.10, 0.15$) by the solid state reaction method. We mixed the elements of Li (99.9%), Zn (99.9%), Cr (99.99%) and As (99%) and slowly heated the mixture to 500°C in evacuated silica tubes, and held for 60 hours before cooling down to room temperature at the rate of $50^\circ\text{C}/\text{h}$. The product was further pressed into pellet, heated to 680°C , and held for 60 more hours. The polycrystals were characterized by X-ray diffraction at room temperature and dc magnetization by Quantum Design SQUID. The electrical resistance was measured on sintered pellets with typical four-probe method.

We show the crystal structure of $\text{Li}_{1.1}\text{Zn}_{1-x}\text{Cr}_x\text{As}$ and the X-ray diffraction patterns in Fig. 1. Bragg peaks from the parent compound LiZnAs can be well indexed by a cubic structure. The single phase is conserved with the doping level up to $x = 0.05$. Small traces of CrAs (an antiferromagnet with $T_N \sim 260$ K [25, 26]) impurities

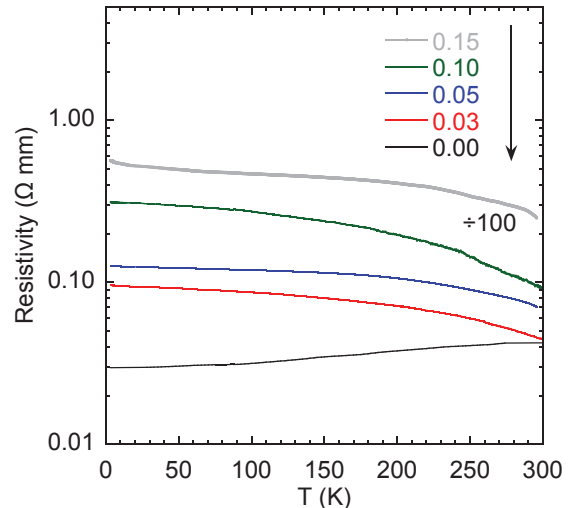


FIG. 2: (Color online) The electrical resistivity of $\text{Li}_{1.1}(\text{Zn}_{1-x}\text{Cr}_x)\text{As}$ with $x = 0, 0.03, 0.05, 0.10, 0.15$; note that the magnitude of $x = 0.15$ is divided by 100 to fit into the window, and the resistivity of $x = 0$ is reproduced from ref. [14].

appear at $x = 0.10$ and 0.15 , as marked by the stars. The lattice constant monotonically decreases from $a = 5.940$ Å for $\text{Li}_{1.1}\text{ZnAs}$ to 5.929 Å for $x = 0.10$, as shown in Fig. 3(e), indicating the successful solid solution of Cr for Zn up to the doping level of 10%.

In Fig. 2, we show the electrical resistivity measured for $\text{Li}_{1.1}\text{Zn}_{1-x}\text{Cr}_x\text{As}$ with $x = 0, 0.03, 0.05, 0.10, 0.15$. For the parent semiconductor LiZnAs (note that Li concentration is exactly 1), it displays a semiconducting behavior within the temperature range of 2 K and 300 K [14]. 10% excess Li readily changes the resistive behavior. As shown in Fig. 2, the resistivity curve of $\text{Li}_{1.1}\text{ZnAs}$ displays a metallic behavior since excess Li provides additional carriers [14]. Interestingly, once 3% Cr is introduced, the resistivity turns to monotonical increase toward lower temperature. This behavior is conserved with the doping level up to 15%. The magnitudes of resistivity at 4 K increase from $0.03 \Omega \text{ mm}$ of $\text{Li}_{1.1}\text{ZnAs}$, to $0.3 \Omega \text{ mm}$ of the sample $\text{Li}_{1.1}\text{Zn}_{0.9}\text{Cr}_{0.1}\text{As}$, and to $55 \Omega \text{ mm}$ of $\text{Li}_{1.1}\text{Zn}_{0.85}\text{Cr}_{0.15}\text{As}$. The type of behavior in Cr doped specimens is likely arising from the scattering of carriers by the magnetic fluctuations through exchange interactions. We do not observe similar insulator to metal transition that takes place at the doping level of $x = 0.03$ for $(\text{Ga}_{1-x}\text{Mn}_x)\text{As}$ [2].

We have also conducted the Hall effect measurements for the sample of $\text{Li}_{1.1}\text{Zn}_{0.95}\text{Cr}_{0.05}\text{As}$ at 200 K. Our results indicate that the carriers are p -type, with a hole concentration of $p \sim 2 \times 10^{20} \text{ cm}^{-3}$. This carrier density is comparable to that of $\text{Li}_{1.1}\text{Zn}_{1-x}\text{Mn}_x\text{As}$ [14] but 3 orders larger than that of $\text{Li}_{1.1}\text{Zn}_{1-x}\text{Mn}_x\text{P}$ [15]. The p -type carriers have also been observed for both $\text{Li}_{1.1}\text{Zn}_{1-x}\text{Mn}_x\text{As}$

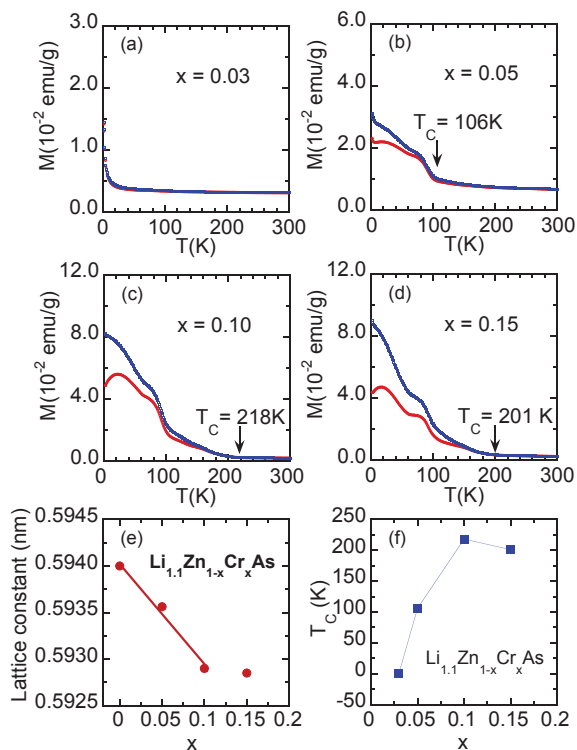


FIG. 3: (Color online) (a)-(d) The magnetization M for $\text{Li}_{1.1}\text{Zn}_{1-x}\text{Cr}_x\text{As}$ with $x = 0.03, 0.05, 0.10, 0.15$ obtained in the zero field cooling (ZFC) and field cooling (FC) in the external field of 1000 Oe; (e) The lattice constant a versus Cr concentration x , the solid line is guide for eyes; (f) T_C versus Cr concentration x .

and $\text{Li}_{1.04}\text{Zn}_{1-x}\text{Mn}_x\text{P}$, which is in contrast with the intuitive expectation that excess Li will render a n -type carriers. There are no convincing experiments to clarify this issue so far. Based on first-principles calculations, Deng et al [15] shows that excess Li^{1+} ions are thermodynamically favored to occupy the Zn^{2+} sites, and each Li^{1+} substitution for Zn^{2+} will introduce a hole carrier.

In Fig. 3, we show the zero-field cooled (ZFC) and field cooled (FC) measurements of the dc -magnetization M of $\text{Li}_{1.1}\text{Zn}_{1-x}\text{Cr}_x\text{As}$ for $B_{ext} = 1000$ Oe. For the doping of $x = 0.03$, we observe a strong increase of M at low temperature, but no splitting is observed between ZFC and FC curves. This indicates that although Cr substitution for Zn introduces local moments, no magnetic ordering is formed. With the doping level increasing to $x = 0.05$, a significant increase in M is observed at the temperature of ~ 106 K, and the ZFC and FC curves split, indicating that the ferromagnetic ordering is taking place. T_C increases to 218 K for the doping level of $x = 0.10$, but decreases to 201 K for $x = 0.15$. We note that for $x = 0.10$ and 0.15, two successive steps at ~ 100 K and ~ 60 K have been observed below T_C . This is possibly arising from either a spin state change of Cr 3d electrons, or the inhomogeneous distribution of Cr atoms in higher levels of Cr doped specimens. We are still working to optimize

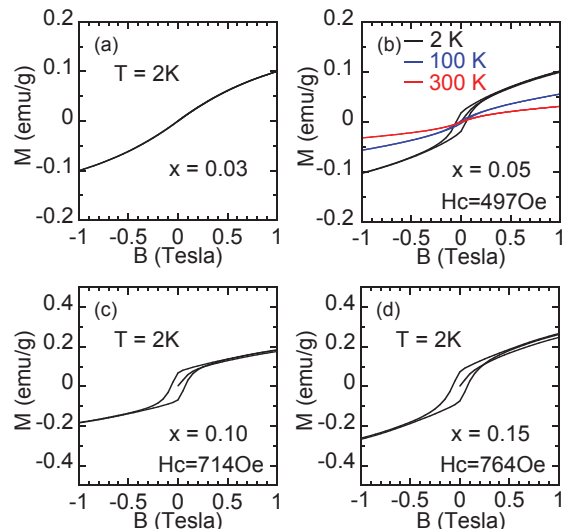


FIG. 4: (Color online) The isothermal magnetization for $\text{Li}_{1.1}\text{Zn}_{1-x}\text{Cr}_x\text{As}$ with $x = 0.03, 0.10, 0.15$ measured at 2 K, and for $x = 0.05$ measured at 2 K, 100 K and 300 K. H_c values are the coercive field at 2 K.

the synthesis condition and to improve the sample homogeneity. None the less, we believe that either reason does not affect the fact that T_C reaches ~ 218 K at the average doping level of 10% Cr. We fit the temperature dependence of M above T_C to a Curie-Weiss law. The effective paramagnetic moment is determined to be $2 \sim 3 \mu_B/\text{Cr}$, which is smaller than the case of $5.1 \pm 0.4 \mu_B$ for $(\text{Ga},\text{Cr})\text{As}$ [23], indicating a likely different spin state in $\text{Li}(\text{Zn},\text{Cr})\text{As}$.

In Fig. 4, we show the isothermal magnetization of $\text{Li}_{1.1}\text{Zn}_{1-x}\text{Cr}_x\text{As}$. For $x = 0.03$, no well formed hysteresis loop is observed even at 2 K, which is consistent with the absence of bifurcation of ZFC and FC curves. For $x = 0.05$, a parallelogram-shaped hysteresis loop with a coercive field of 497 Oe is observed at 2 K. The coercive field decreases to 177 Oe at 100 K and becomes zero at 300 K. For $x = 0.10$ and 0.15, the coercive fields at 2 K are 714 Oe and 764 Oe, respectively, which are larger than $\sim 50 - 100$ Oe of the same cubic structural $\text{Li}_{1.1}(\text{Zn}_{0.97}\text{Mn}_{0.03})\text{As}$ [14], $\text{Li}_{1.1}(\text{Zn}_{0.97}\text{Mn}_{0.03})\text{P}$ [15] and $(\text{Ga}_{0.965}\text{Mn}_{0.035})\text{As}$ [1].

In diluted magnetic systems, the magnetic impurities can easily give rise to spurious features of “ferromagnetism”, such as the bifurcation of ZFC and FC curves and hysteresis loops [27, 28]. For the $x = 0.05$ specimen with $T_C = 106$ K, the phase is pure, as shown in Fig. 1(c). We detected tiny traces of CrAs impurities for $x = 0.10$ and 0.15 samples. However, CrAs is an antiferromagnet with $T_N \sim 260$ K [25, 26], which does not likely contribute to the observed remanent magnetization in these bulk form polycrystals. In the $\text{Li}(\text{Zn},\text{Cr})\text{As}$ system, the ordering temperature T_f systematically increases with higher Cr doping levels, along with the successful solid solution of Cr for Zn as shown in Fig. 3(e), indicating that the

magnetic ordering is truly arising from the Cr atoms that substituted for the Zn atoms in ionic sites. We would observe a single transition temperature for all doping levels if the magnetic ordering arises from the same type of magnetic impurity source or the uncompensated spins as observed in thin films [29]

In general, the bifurcation of ZFC and FC curves and the hysteresis loops can be found not only in regular ferromagnets [30] but also in spin glasses [31]. One decisive technique to distinguish the two cases is neutron scattering, which can resolve spatial spin correlations. We have conducted neutron diffraction experiment on $(\text{Ba}_{0.7}\text{K}_{0.3})(\text{Zn}_{0.9}\text{Mn}_{0.1})_2\text{As}_2$ [19] and $(\text{La}_{0.9}\text{Sr}_{0.1})(\text{Zn}_{0.9}\text{Mn}_{0.1})\text{AsO}$ [32] polycrystalline DMS specimens. Unfortunately, it is still difficult to decouple the magnetic and structural Bragg peaks even at 6 K due to the spatially dilute Mn moments. We are making efforts to grow single crystals for high resolution neutron scattering experiments at this stage.

In summary, we reported the synthesis and characterization of bulk form diluted magnetic semiconductors $\text{Li}(\text{Zn},\text{Cr})\text{As}$ with the ordering temperature as high as \sim

218 K. It is the first time that Cr atoms are doped and a ferromagnetic ordering is observed in a I-II-V semiconductor. The ferromagnetic ordering is arising from the Cr atoms that substituted for Zn in ionic sites, and the Cr spins are mediated by the carriers from excess 10 % Li. $\text{Li}(\text{Zn},\text{Cr})\text{As}$ therefore represents a Cr induced DMS family that has the advantage of decoupling of carrier and spins, whose spins are introduced by Cr substitution for Zn and carriers are created by adding extra Li. Our fabrication of new $\text{Li}(\text{Zn},\text{Cr})\text{As}$ DMSs provides another DMS system for the future research of precise controlling carriers/spins and their individual influence to the ferromagnetic ordering.

The work at Zhejiang University was supported by National Basic Research Program of China (No. 2011CBA00103, No. 2014CB921203), NSFC (No. 11274268); F.L. Ning acknowledges partial support by the US NSF PIRE (Partnership for International Research and Education: OISE-0968226) and helpful discussion with J.H. Zhao, J.H. Dai, C. Cao, C.Q. Jin and Y.J. Uemura.

-
- [1] H. Ohno, A. Shen, F. Matsukura, A. Oiwa, A. Endo, S. Katsumoto, and Y. Iye, *Appl. Phys. Lett.* **69**, 363 (1996).
- [2] T. Jungwirth, J. Sinova, J. Masek, J. Kucera, and A.H. MacDonald, *Rev. Mod. Phys.* **78**, 809 (2006).
- [3] T. Dietl, *Nature Materials* **9**, 965 (2010).
- [4] I. Zutic, J. Fabian, and S. Das Sarma, *Rev. Mod. Phys.* **76**, 323 (2004).
- [5] L. Chen, S. Yan, P.F. Xu, W.Z. Wang, J.J. Deng, X. Qian, Y. Ji, J.H. Zhao, *Appl. Phys. Lett.* **95**, 182505 (2009).
- [6] L. Chen, X. Yang, F.H. Yang, J.H. Zhao, J. Misuraca, P. Xiong and S.V. Molnar, *Nano Lett.* **11**, 2584 (2011).
- [7] A. Pajaczkowska, *Prog. Cryst. Growth Charact.* **1**, 289 (1978).
- [8] J.K. Furdyna, *J. Appl. Phys.* **64**, R29 (1988).
- [9] T. Wojtowicz, T. Dietl, M. Sawicki, W. Plesiewicz, and J. Jaroszynski, *Phys. Rev. Lett.* **56**, 2419 (1986).
- [10] H. Morkoc, S. Strite, G. B. Gao, M. E. Lin, B. Sverdlov, and M. Burns, *J. Appl. Phys.* **76**, 1363 (1994).
- [11] P.M. Shand, A.D. Christianson, T.M. Pekarek, L.S. Martinson, J.W. Schweitzer, I. Miotkowski, and B.C. Crooker, *Phys. Rev. B* **58**, 12876 (1998).
- [12] J. Masek, J. Kudrnovsky, F. Maca, B.L. Gallagher, R.P. Campion, D.H. Gregory, and T. Jungwirth, *Phys. Rev. Lett.* **98**, 067202 (2007).
- [13] R. Bacewicz, and T.F. Ciszek, *Appl. Phys. Lett.* **52**, 1150 (1988).
- [14] Z. Deng, C.Q. Jin, Q.Q. Liu, X.C. Wang, J.L. Zhu, S.M. Feng, L.C. Chen, R.C. Yu, C. Arguello, T. Goko, F.L. Ning, J.S. Zhang, Y.Y. Wang, A.A. Aczel, T. Munsie, T.J. Williams, G.M. Luke, T. Kakeshita, S. Uchida, W. Higemoto, T.U. Ito, B. Gu, S. Maekawa, G.D. Morris and Y.J. Uemura, *Nature Communications* **2**, 422 (2011).
- [15] Z. Deng, K. Zhao, B. Gu, W. Han, J.L. Zhu, X.C. Wang, X. Li, Q.Q. Liu, R.C. Yu, T. Goko, B. Frandsen, L. Liu, J.S. Zhang, Y.Y. Wang, F.L. Ning, S. Maekawa, Y.J. Uemura and C.Q. Jin, *Phys. Rev. B* **88**, 081203(R) (2013).
- [16] C. Ding, C. Qin, H.Y. Man, T. Imai and F.L. Ning, *Phys. Rev. B* **88**, 041108(R) (2013).
- [17] C. Ding, H.Y. Man, C. Qin, J.C. Lu, Y.L. Sun, Q. Wang, B.Q. Yu, C.M. Feng, T. Goko, C.J. Arguello, L. Liu, B.A. Frandsen, Y.J. Uemura, H.D. Wang, H. Luetkens, E. Morenzoni, W. Han, C.Q. Jin, T. Munsie, T.J. Williams, R.M. D'Ortenzio, T. Medina, G.M. Luke, T. Imai, F.L. Ning, *Phys. Rev. B* **88**, 041102(R) (2013).
- [18] X.J. Yang, Y.K. Li, C.Y. Shen, B.Q. Si, Y.L. Sun, Q. Tao, G.H. Cao, Z.A. Xu, and F.C. Zhang, *Appl. Phys. Lett.* **103**, 022410 (2013).
- [19] K. Zhao, Z. Deng, X.C. Wang, W. Han, J.L. Zhu, X. Li, Q.Q. Liu, R.C. Yu, T. Goko, B. Frandsen, L. Liu, F.L. Ning, Y.J. Uemura, H. Dabkowska, G.M. Luke, H. Luetkens, E. Morenzoni, S.R. Dunsiger, A. Senyshyn, P. Böni and C.Q. Jin, *Nature Communications* **4**, 1442 (2013).
- [20] H. Saito, V. Zayets, S. Yamagata and K. Ando, *Phys. Rev. Lett.* **90**, 207202 (2003).
- [21] J. Lu, H.J. Meng, K. Zhu, L. Chen, P.F. Xu Z. Xie and J.H. Zhao, *Europhysics Letters* **89**, 67003 (2010).
- [22] H. Wu, H.D. Gan, H.Z. Zheng, J. Lu, H. Zhu, Y. Ji G.R. Li and J.H. Zhao, *Solid State Communications* **151**, 456 (2011).
- [23] H. Saito, W. Zaets, R. Akimoto, K. Ando, Y. Mishima and M. Tanaka, *J. Appl. Physics* **89**, 7392 (2001).
- [24] S. Kuroda, N. Nishizawa, K. Takita, M. Mitome, Y. Bando, K. Osuch and T. Dietl, *Nature Materials* **6**, 440 (2007).
- [25] K. Selte, A. Kjekshus, W.E. Jamison A.F. Andresen and J. Engebretsen, *Acta Chem. Scand.* **25**, 1703 (1971).
- [26] A. Selte, H. Boller, and E.F. Bertaut, *J. Phys. Chem. Solids* **35**, 1139 (1974).

- [27] N.Samarth, Nature Materials **9**, 955 (2010).
- [28] S.Chambers, Nature Materials **9**, 956 (2010).
- [29] T. Dietl, T. Andrearczyk, A. Lipinsa, M. Kiecana, Maureen Tay, and Yihong Wu, Phys. Rev. B **76**, 155312 (2007).
- [30] N.W. Ashcroft and N.D. Mermin, Solid State Physics **Holt, Rinehart and Winston, 1976.**
- [31] K.H. Fischer and J.A. Hertz, **Spin Glasses Cambridge University Press, 1991.**
- [32] J.C. Lu, H.Y. Man, C. Ding, Q. Wang, B.Q. Yu, S.L. Guo, Y.J. Uemura, W. Han, C.Q. Jin, H.D. Wang, B. Chen and F.L. Ning, Europhysics Letters **103**, 67011 (2013).